

# Merging the MODIS and Landsat Terrestrial Latent Heat Flux Products Using the Multiresolution Tree Method

Jia Xu<sup>1</sup>, Yunjun Yao, Shunlin Liang<sup>2</sup>, *Fellow, IEEE*, Shaomin Liu, Joshua B. Fisher, Kun Jia<sup>3</sup>, Xiaotong Zhang<sup>4</sup>, Yi Lin<sup>5</sup>, Lilin Zhang, and Xiaowei Chen

**Abstract**—The accurate estimation of the terrestrial latent heat flux (LE) from satellite observations at high spatial and temporal scales plays an important role in the assessment of the water and heat exchange between the earth’s surface and the atmosphere. Although a variety of data fusion methods have been proposed to merge different LE products for more reliable estimates, most of them have ignored the spatiotemporal consistency of LE products across different resolutions. In this paper, we apply the multiresolution tree (MRT) method to improve the accuracy and reduce the inconsistency between the Moderate Resolution Imaging Spectroradiometer (MODIS) LE (MOD16) product and the Landsat-based LE product at different resolutions. Eddy covariance (EC) ground measurements at five sites, MODIS and Landsat images from January 2005 to December 2005 in the north central USA, are used to evaluate the performance of the MRT method. The results show that the MRT method can improve the accuracy of the original LE products (MOD16 and Landsat), and it has the potential to significantly reduce the uncertainty and inconsistency of these products. The bias decreased by 38.3% on average, and the root-mean-square error (RMSE) decreased by approximately 49.2% after the MRT was applied at each scale. Further studies are still required to make the MRT method more universal on a variety of land cover types for long-time periods.

**Index Terms**—Eddy covariance, Landsat data, MODIS, multiresolution tree (MRT), terrestrial latent heat flux (LE).

Manuscript received April 27, 2018; revised August 2, 2018; accepted October 4, 2018. Date of publication November 9, 2018; date of current version April 22, 2019. This work was supported in part by the National Natural Science Foundation of China under Grant 41671331, in part by the National Key Research and Development Program of China under Grant 2016YFA0600102, and in part by the California Institute of Technology. The work of J. B. Fisher was supported by NASA: SUSMAP, IDS, INCA, and ECOSTRESS. (*Corresponding author: Yunjun Yao.*)

J. Xu, Y. Yao, K. Jia, X. Zhang, L. Zhang, and X. Chen are with the State Key Laboratory of Remote Sensing Science, Faculty of Geographical Science, Beijing Normal University, Beijing 100875, China (e-mail: diamond1201@sina.cn; boyyunjun@163.com; jiakun@bnu.edu.cn; xtngzhang@bnu.edu.cn; 595905322@qq.com; 18368091857@163.com).

S. Liang is with the Department of Geographical Sciences, University of Maryland, College Park, MD 20742 USA (e-mail: sliang@umd.edu).

S. Liu is with the State Key Laboratory of Earth Surface Processes and Resource Ecology, Faculty of Geographical Science, Beijing Normal University, Beijing 100875, China (e-mail: smliu@bnu.edu.cn).

J. B. Fisher is with the Jet Propulsion Laboratory, California Institute of Technology, Pasadena, CA 91109 USA (e-mail: joshbfisher@gmail.com).

Y. Lin is with the School of Earth and Space Sciences, Peking University, Beijing 100871, China (e-mail: yi.lin@pku.edu.cn).

Color versions of one or more of the figures in this paper are available online at <http://ieeexplore.ieee.org>.

Digital Object Identifier 10.1109/TGRS.2018.2877807

## I. INTRODUCTION

THE terrestrial latent heat flux (LE), which is the heat flux from the earth’s surface to the atmosphere pertaining to the surface soil evaporation, vegetation interception, and vegetation transpiration [1]–[5], is a major component of the global and regional surface energy redistribution and the water cycle. It is difficult to accurately measure terrestrial LE because LE generally suffers from heterogeneity across the land surface, complicated biophysical feedback processes, and complex environmental controls [2], [6], [7]. Ground-based observation methods, such as the energy balance Bowen ratio (EBBR) method [8]–[10] and the eddy covariance (EC) method [11]–[13], are widely used for accurately measuring the continuous LE at the point scale. However, the scale mismatch between point and regional scales hinders such observations as representing LE at regional and global scales [14]–[17].

Satellite remote sensing provides observations of terrestrial biophysical variables for estimating LE, and many methods have been proposed to estimate LE during the past several decades. However, satellite-based LE products can utilize more than just remote sensing observations and can also utilize meteorological data sets and LE algorithms. Due to the errors in the meteorological inputs, the differences in satellite-based biophysical variables derived from different sensors, and the influence of the physical structures of different LE algorithms [18], the differences among individual LE products vary considerably [19]. In addition, current satellite-based LE products have either high spatial resolution and low temporal resolution or coarse spatial resolution and high temporal resolution [20]. While there are very few satellite-based LE products with both high spatial resolution and high temporal resolution, the Moderate Resolution Imaging Spectroradiometer (MODIS) LE product (MOD16) can cover the global surface with moderate spatial resolution (~1 km) and temporal resolution (8 days) [21], [22]. However, many studies have revealed the large uncertainties and the low accuracy of the MOD16 product. For instance, the MOD16 product was found to have large uncertainties [23] compared with other process-based models, such as the revised Penman–Monteith (PM) model [7] and the Priestley–Taylor Jet Propulsion Laboratory (PT-JPL) model [24]. The results also showed that the MOD16 product underestimated LE in savanna and woodland

ecosystems [25], and the croplands and grasslands in East Asia [26]. In addition, the 1 km LE estimates tend to be inaccurate and are not applicable at the field, local, or basin scales because of a high level of spatial heterogeneity of land cover within a pixel. Fortunately, the Landsat multispectral data record from the Thematic Mapper (TM) and the Enhanced Thematic Mapper Plus (ETM+) are estimable data sources for producing LE products at high spatial resolution ( $\sim 30$  m) [27], and they are widely used to estimate LE based on physical mechanisms or empirical algorithms [28], [29]. They are also able to bridge the gap between current LE products with coarse resolution and point-based field measurements and validate coarse resolution data. However, because the temporal resolution of the Landsat data is relatively lower (16 days) than that of the MOD16 product and Landsat images are periodically contaminated by clouds, this temporal resolution is often unattainable for many areas and insufficient to meet the needs of accurate LE mapping. Moreover, some Landsat LE products contained uncertainties as well. For example, the Mapping Evapotranspiration at high resolution with internalized calibration (METRIC) model-driven Landsat LE product was underestimated by 11% compared with the reference LE information from the energy-budget corrected EC method [30].

To reduce the uncertainties among different LE products, many data merging methods have been proposed to merge multiple LE data sets for improving terrestrial LE estimations. Previous studies revealed that the merged LE is more reliable and accurate than the LE result from an individual data set [31], [32]. For instance, Yao *et al.* [33] used the Bayesian model averaging (BMA) method by merging five LE products to enhance the daily LE estimation with smaller root-mean-square errors (RMSEs) than those of the individual LE products. Although previous studies have shown that the BMA method is more reliable and capable than the simple model averaging (SMA) method, the weights for the individual data sets using the BMA method are highly dependent on the samples of the EC ground measurements of LE, which limits its wide application [34]. Similarly, Feng *et al.* [35] found that an empirical orthogonal function (EOF) method is efficient to merge the two satellite-based LE data sets to improve the consistency and reduce the uncertainties in LE estimates. However, the EOF method failed to resolve the inconsistent resolution among different LE products. Similarly, Wang and Liang [36] applied the optimal interpolation (OI) method to integrate multiple LAI products. The inputs from MODIS and CYCLOPES are at the same resolutions ( $\sim 1$  km) as well, and even the slow computation limits its application. Overall, these merging methods ignore the spatial and temporal consistency across different resolutions and require higher computational efficiency.

Recently, a multiresolution tree (MRT) method has been applied to make consistent predictions across different spatial resolutions using the hypothesis that a statistical model is autoregressive in its levels of resolution [37]. The MRT method has been widely used on large data sets to estimate satellite-based variables across different spatial resolutions and to overcome the computational complexity that other existing

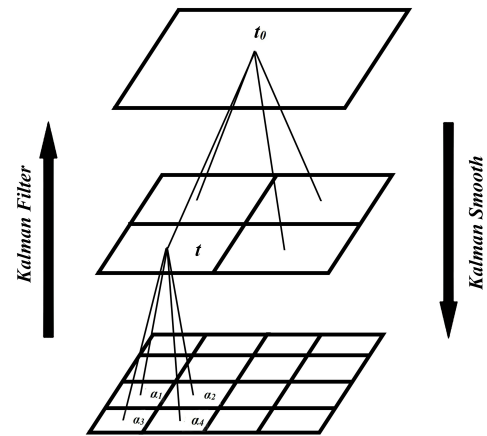


Fig. 1. Framework of the MRT tree structure. Node  $t$  shows the relationship between its parent  $t_0$ , and its children  $a_1$ ,  $a_2$ ,  $a_3$ , and  $a_4$ . In this paper, the Landsat LE product serves as the leaf node, and the MOD16 LE product is in the middle of the tree.

methods may have [38]–[40]. For example, the MRT method has been applied to resolve some geoscience issues, such as the assimilation of soil moisture [41] and albedo data sets at different resolutions [42]. Wang and Liang [36] applied both the MRT and optimal OI methods to merge LAI products from MODIS and Multi-angle Imaging SpectroRadiometer (MISR) and proved that the MRT method possessed higher computational efficiency and improved the quality of LAI products. Because of its time efficiency and capability of generating interpolations with minimal bias across different spatial resolutions, this method can be used to merge terrestrial LE products from multiple satellite data sets with different spatial resolutions. However, there is a lack of similar studies on improving terrestrial LE estimates based on the MRT method for monitoring the dynamics of the regional water budget.

In this paper, we use the MRT method to merge two satellite-based LE products (MODIS and Landsat LE product) to generate consistent LE data sets at different spatial resolutions. The objectives of this paper are threefold: 1) to evaluate MODIS and Landsat LE products using AmeriFlux measurements from five flux tower sites in the north central USA; 2) to merge two satellite-derived LE products (MODIS and Landsat LE products) using the MRT method to eliminate the inconsistency of different LE products; and 3) to compare MODIS and Landsat LE products before and after fusion.

## II. METHOD

The basic concept of MRT is a linear tree structure and the data at different spatial resolutions are autoregressive (Fig. 1).

The linear state model can be written in a scalar version as follows [43]:

$$x(t) = A(t)x(t\gamma) + w(t) \quad (1)$$

where  $x(t)$  and  $x(t\gamma)$  represent the variable of interest at child scale (fine scale)  $t$  and its parent scale (coarse scale)  $t\gamma$ , respectively.  $w(t)$  is the state transition noise that follows the Gaussian distribution  $N(0, Q(t))$ .  $A(t)$  is the state transition

matrix from the parent scale  $t\gamma$  to its child node and is generally assigned to an identity matrix [44], [45]. There is a similar equation that transfers the variable from fine-scale  $t$  to the coarse-scale  $t\gamma$ . [43]

Except for the state transition model, an observation equation is also required in this method by linking the satellite-based products to the variable of interest

$$y(t) = Hx(t) + v(t) \quad (2)$$

where  $y(t)$  is the satellite data with an observation noise  $v(t)$  that follows the Gaussian distribution  $N(0, R(t))$ . Because both the satellite data and the variable of interest are LE and the same area is used, the observation matrix  $H$  is taken as the identity matrix. The two variables from the fine scale to coarse scale are previously processed: the state transition predicted values  $\hat{x}(t\gamma|t)$  using the observations to the scale  $t$  and the observed values  $y(t\gamma)$  at scale  $t\gamma$ . A Kalman filter is used to combine this information [46]

$$\hat{x}(t\gamma|t\gamma) = \hat{x}(t\gamma|t) + K(t\gamma)(y(t\gamma) - H\hat{x}(t\gamma|t)). \quad (3)$$

Here,  $\hat{x}(t\gamma|t\gamma)$  is the optimal estimator at scale  $t\gamma$  by incorporating observations up to scale  $t$ .  $K(t)$  is the Kalman gain and is taken by the following [46], [47]:

$$K(t\gamma) = P(t\gamma|t)HV^{-1}(t\gamma) \quad (4)$$

where  $V(t)$  is the innovation covariance

$$V(t\gamma) = HP(t\gamma|t)H^T + R(t\gamma). \quad (5)$$

Every child node provides an estimate to its parent node and the optimal estimator  $\hat{x}(t\gamma|t\gamma)$  consists of a weighted sum of the estimates of its children. The weight of the estimate is controlled by the variance  $P^*(t)$ , which indicates that the larger the uncertainty of an estimate, the smaller the effect of that estimate in the merging process. Through (1)–(5), we obtained the optimal estimates at each scale. To take full advantage of the fine-scale data and the coarse-scale data, the Kalman smooth is used to obtain the final predicted value  $\hat{x}'(t)$  and to integrate the variable at each resolution. The Kalman smooth is given as follows [43], [46], [47]:

$$\hat{x}'(t) = \hat{x}(t|t) + J(t)(\hat{x}'(t\gamma) - \hat{x}(t\gamma|t)) \quad (6)$$

$$J(t) = F(t)P(t|t)/P(t\gamma|t) \quad (7)$$

where  $J(t)$  is a weighted coefficient.

There are two steps in the MRT method: the “leaves to root” Kalman filter and the “root to leaves” Kalman smooth. Starting at the finest scale, the ascending propagation is recursively updated until arriving at the root node. After the Kalman filter process finishing, the descending propagation, that is, the Kalman smooth starts at the next scale of the root scale and continues to the finest scale. The Kalman filter aims to fill in the gaps at each scale and provides the finer information to the coarser scale. The Kalman smooth updates the state estimation with the information at a coarser scale. After the two steps, the data sets at different resolutions can be smooth and consistent. Further details of the MRT method can be found in Vyver *et al.* [48]

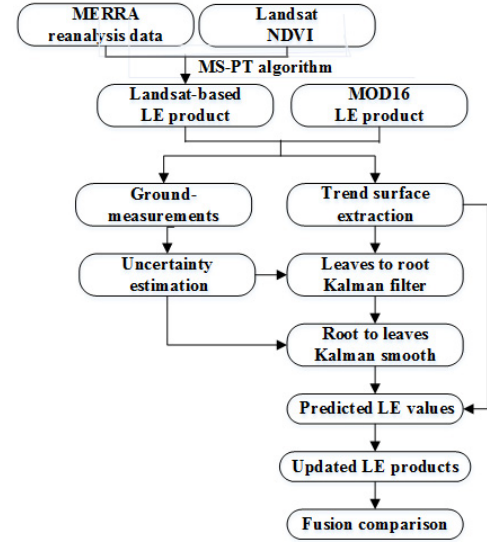


Fig. 2. Flowchart of the MRT fusion procedure from different satellite-based LE products.

To implement the MRT method, our study includes several steps, which are shown in Fig. 2. First, to evaluate the data uncertainties of two satellite-based LE products, we use the ground measurements to validate and provide additional accurate information by comparing different satellite products. Second, there is one basic assumption that the variables used in the MRT method are zero mean in the spatial process, and hence the surface extraction of the two satellite products is implemented. Based on the detrending products, we calculate the variance  $Q(t)$  for the leaves and obtain the observation error  $v(t)$  using the standard deviation of the relative difference between the finest resolution product and the ground measurements. To obtain the variance  $R(t)$  other than the child nodes, we calculate the relative difference between the parent nodes and the aggregated data from their child nodes. Third, to obtain and update the LE data at each scale involved, the “leaves to root” Kalman filter and the “root to leaves” Kalman smooth are implemented. After that, we add the updated spatial residual back to the trend surface to obtain the optimal LE fusion data at all levels. Finally, the MRT performance is compared with several indicators for evaluation before and after MRT.

### III. EXPERIMENTAL DATA AND PREPROCESSING

#### A. Study Area

The study area is located in northern Wisconsin, a state in the USA (Fig. 3).

A subset of an approximately  $45 \text{ km} \times 45 \text{ km}$  area was extracted from two satellite-based LE products in the Universal Transverse Mercator (UTM) projection for 2005. The images were selected based on the availability of the two LE products and those that suffered less from cloud contamination in this paper. The land cover types are 48.51% mixed forest (MF), 16.11% deciduous broadleaf forest (DBF), 14.31% grassland (GRA), 10.19% open and closed shrubland (SHR), 5.89% savannas and woody savannas (SAW), 2.22% cropland (CRO),

TABLE I  
LOCATIONS OF THE 5 FLUX TOWERS

Site ID	Site name	Lat, Lon	IGBP	Elevation (m)	Average annual LE (W/m <sup>2</sup> )	Measurement method	Project	Time period
US-Los	Lost Creek	46.082°N 89.980°W	SHR	480	34.92	ECOR	AmeriFlux	2001-2005
US-Syv	Sylvania Wilderness	46.242°N 89.348°W	MF	540	40.90	ECOR	AmeriFlux	2001-2008
US-WCr	Willow Creek	45.806°N 90.080°W	DBF	520	43.09	ECOR	AmeriFlux	2000-2006
US-Bo1	Bondville	40.006°N 88.290°W	CRO	219	55.80	ECOR	AmeriFlux	1996-2010
US-Bo2	Bondville Companion Site	40.009°N 88.290°W	CRO	219	58.65	ECOR	AmeriFlux	2004-2008

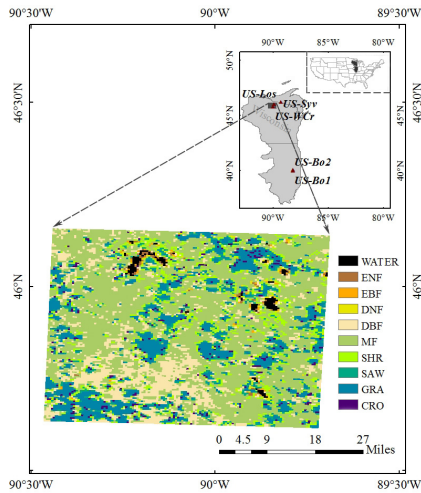


Fig. 3. Map of land cover types from MODIS (IGBP classification) and the locations of the EC towers.

1.08% water, 0.64% deciduous needleleaf forest (DNF), 0.57% evergreen needleleaf forest (ENF), and 0.48% evergreen broadleaf forest (EBF), which are from the MODIS land cover type product (MCD12Q1) with 500 m resolution [49]. MODIS tile h11v04 and Landsat TM scene p25r28 were selected to match with each other.

As shown in Table I, ground measurements from five EC towers are based on the eddy covariance (ECOR) method and are provided by AmeriFlux. They cover four types of vegetation, including SHR, MF, DBF, and CRO. The selected sites differ in land cover types, elevations, and climatological characteristics. The half-hour data included the surface net radiation ( $R_n$ ), shortwave solar radiation ( $R_s$ ), soil heat flux ( $G$ ), LE, sensible heat flux ( $H$ ), air temperature ( $T_a$ ), relative humidity (RH), and atmospheric water pressure ( $e$ ). We linearly aggregated the half-hour turbulent surface heat fluxes and other climate parameters into daily and monthly means. Because of the energy nonclosure problem [11], [50], we used the following method, which was proposed by Twine *et al.* [50], to correct the measured LE values at these sites:

$$LE_{cor} = (R_n - G)/(LE_{ori} + H_{ori}) \times LE_{ori} \quad (8)$$

where  $LE_{cor}$  is the corrected LE and  $LE_{ori}$  and  $H_{ori}$  are the uncorrected LE and  $H$ , respectively.

## B. Satellite-Based LE Products

1) *MODIS LE Product*: The MODIS LE product (MOD16) is produced based on an improved (PM) algorithm [1] according to a beta version [21] after being adapted by Cleugh *et al.* [51]. The MOD16 algorithm calculates the LE as the sum of daytime and nighttime components, divides the canopy and soil into wet and dry components, and modifies the vegetation cover with FPAR (fraction of absorbed photosynthetically active radiation) derived from MOD15A2 [22]. The MOD16 product is composited every 8 days with 1 km spatial resolution and data from 2005 that are used in this paper. To merge each node of different resolutions in the same projection, a reprojection of the MOD16 was processed from the sinusoidal projection into the UTM coordinate system to match with that of the Landsat-based LE product. The real grid size of the nominal 1 km sinusoidal pixel is 926.6 m and is resampled to the 900 m pixel size using the bilinear interpolation method [52] to match it with the 30 m pixel size of the Landsat TM scenes.

2) *Landsat-Based LE Product*: The Landsat L1T data are calibrated and projected in the UTM projection, and the actual pixel size is 30 m taken over a period of 16 days. To eliminate the radiation error and obtain the surface reflectance, the atmospheric correction is required for the Landsat L1T data using the Landsat ecosystem disturbance adaptive processing system (LEDAPS) tool [53]. Only the Landsat scenes with less than 30% cloudy pixels were selected to reduce the effect of the cloud contamination.

We produced the Landsat-based LE product using the modified satellite-based Priestley–Taylor (MS-PT) algorithm developed by Yao *et al.* [54]. This algorithm was developed on the Priestley–Taylor (PT) model's basis [55], which uses the apparent inertia (ATI) derived from the diurnal air temperature range (DT) for parameterizing the surface soil moisture constraints. The forcing data requires only the net radiation ( $R_n$ ), the air temperature ( $T_a$ ), the DT from the modern era retrospective analysis for research and applications (MERRA) meteorological reanalysis data, and the NDVI from the Landsat data for 2005. A spatial resolution resample of 30 m for the MERRA data was implemented by using the method described by Zhao *et al.* [56], which improves the accuracy of interpolation by removing the sharp changes from one side of the boundary to the other [56]. The details of the MS-PT algorithm are given in the Appendix.

C. Assessment Method

We used three different statistical criteria to evaluate the performance of the MRT method in this paper: the root-mean-square error (RMSE), the relative RMSE in percentage (RMSE%), and the bias. The RMSE is calculated as the square root of the average value of the differences between the observed and predicted LE values. The lower the RMSE is, the more reliable the model’s performance is. The RMSE% demonstrates the relative error and is capable of capturing outliers of MRT performance. Bias reflects the average value of the differences between the observed and predicted LE values. The results were also compared with histograms before and after fusion. The metrics are calculated as follows:

$$RMSE = \sqrt{\frac{\sum_{i=1}^n (X_{obs,i} - X_{model,i})^2}{n}} \quad (9)$$

$$RMSE\% = \sqrt{\frac{\sum_{i=1}^n \left(\frac{X_{obs,i} - X_{model,i}}{X_{obs,i}}\right)^2}{n}} \quad (10)$$

$$Bias = \frac{\sum_{i=1}^n (X_{obs,i} - X_{model,i})}{n} \quad (11)$$

where  $X_{obs}$  and  $X_{model}$  are the observed and estimated LE values, respectively.

IV. RESULTS ANALYSIS

A. Evaluation of Satellite-Derived LE at the Flux Tower Sites

We compare two LE products with the ground measurements for five AmeriFlux sites for 2005 using time series to demonstrate the accuracy of the information. The uncertainties among different LE products spatially and temporally vary greatly [57], [58]. Due to the limitation of the temporal resolution and the Landsat product missing at some sites, such validation may not be able to evaluate the uncertainties, and we focus on prototyping the merging algorithm in this paper.

The comparison between the two LE products and the EC ground measurements showed that the Landsat LE product provided better matches with the ground measurements than that of the MOD16 since the finer spatial resolution of the Landsat data are more suitable for matching with the EC ground measurements (Fig. 4). In terms of the uncertainty of the Landsat LE product, cloud contamination may be the possible reason, even though the atmospheric correction has been implemented using the LEDAPS tool. The MOD16 overestimated the LE in winter and underestimated the LE in the vegetation growing period by approximately 10–20 W/m<sup>2</sup>. Perhaps the biophysical processes and the pixel heterogeneity at different times and locations can affect the accuracy of the MOD16 [22]. Moreover, there was a significant scale difference between the MOD16 and the ground measurements since the MOD16 tended to underestimate in the vegetation growing season when compared directly with the ground measurements [59].

Fig. 5 shows the scatterplots of the comparison between the satellite-derived LE products (the Landsat-based LE product and the MOD16 LE product) and the ground measurements for 2005. The outliers contaminated by cloud shadows

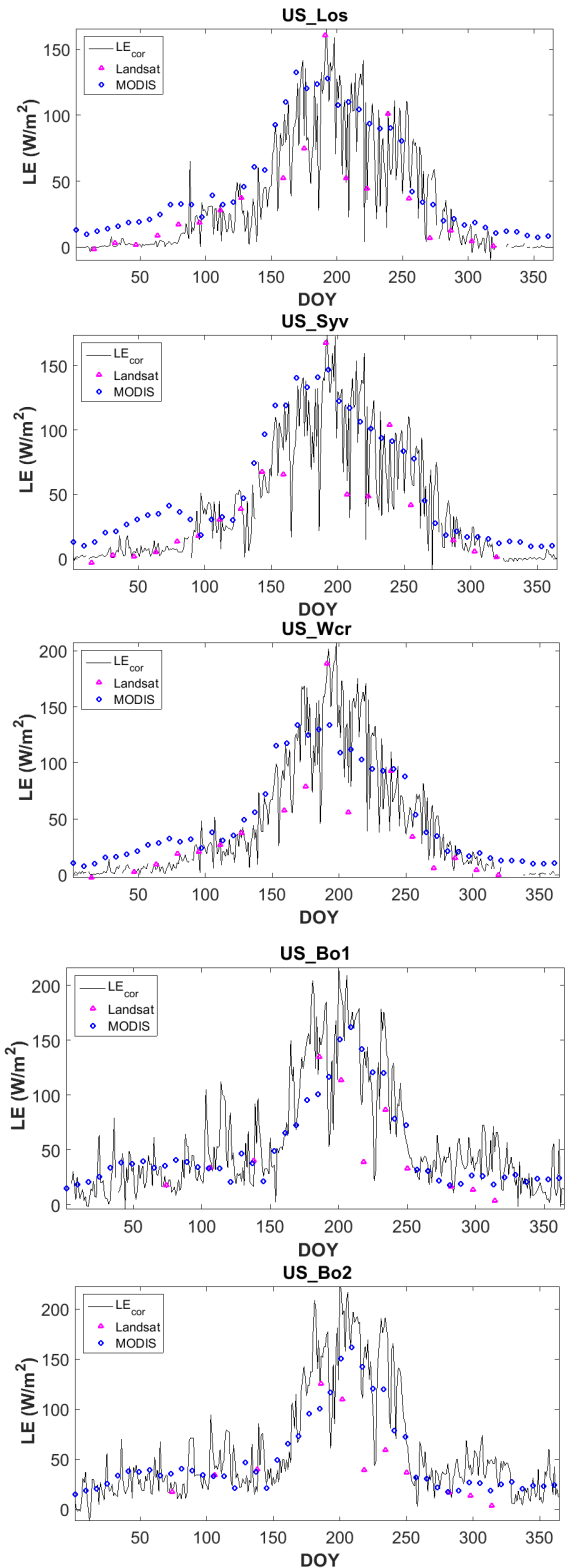


Fig. 4. Intercomparison of the Landsat and MOD16 LE products on time series for 2005 for five flux tower sites. LE\_cor refers to the corrected ground measurements.

were removed. One notices that the Landsat estimated the LE better with  $R^2$  of 0.866 and RMSE of 17.317 W/m<sup>2</sup> than the MOD16 with  $R^2$  of 0.626 and RMSE of 27.6 W/m<sup>2</sup>. Therefore, we used the standard deviation of the relative error

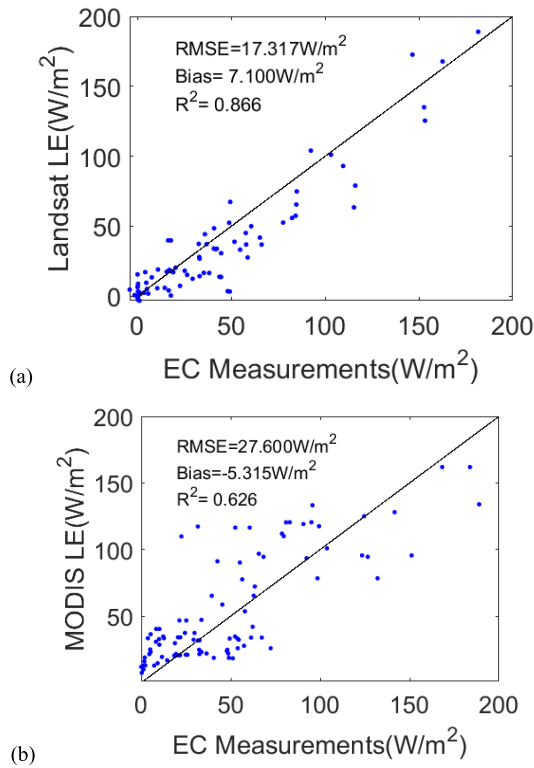


Fig. 5. Scatterplots of the comparison of the Landsat and MOD16 data using the ground measurements. (a) Landsat. (b) MOD16.

of the Landsat data as the observation error  $v(t)$ . However, it might be unreasonable to directly evaluate the MOD16 using the ground measurements because of the large differences in the spatial resolutions. To obtain the observation error of the MOD16, the Landsat data were aggregated to match the grid size of the MOD16 and to estimate the relative error for each scene. To implement the MRT method, we assumed that the pixels of the study area had invariant errors within different temporal and spatial variations.

### B. MRT-Based Satellite-Derived LE Product Fusion

There is a basic assumption in the MRT method that the data of the tree structure at each scale is zero mean. However, the original LE products cannot satisfy the requirement, and the spatial trend surface is required to be extracted from the original data. To obtain the zero mean detrending data, a simple average [60] was applied, and the estimated detrending data were then added back into the trend surface to generate the merged LE products.

The two LE products and the corresponding merged results were compared on time series from DOY 97 to DOY 121 and DOY 233 to DOY 241 based on the availability of clear scenes of the two LE products (Fig. 6). To avoid the potential error, the pixels contaminated by clouds and water bodies were excluded using a dark blue color in the Landsat and the MOD16 products. Different from other common merging methods, the MRT method provides separate results at different spatial resolutions. One notices that the same Landsat data may be shared by two adjacent MODIS scenes.

Data at finer resolution usually provide more information of the random spatial processes than the coarser resolution, and the average information carried by the coarser resolution data can also fill the gaps for the finer resolution data. Compared with the original products, both products after data fusion tended to be consistent across different scales, and the differences between the satellite products were greatly reduced. The contaminated pixels or data gaps of the Landsat data were effectively filled, particularly in DOY 97. For the MOD16, the areas with overestimated or underestimated LEs were smoothed after the MRT and became much closer to Landsat than before. The obvious outliers, such as the yellow spots in DOY 97, DOY 105, and DOY 103, were also eliminated. Since Landsat provides coarser resolution data with finer information for capturing the LE trends in the spatial domain, the MOD16 LE values changed greatly, and the Landsat LE values were adjusted lower. However, the abnormal LE values in DOY 105 imply that the MRT method is limited if the inputs have large differences. The principle of the MRT method is adjusting the pixel values according to the uncertainties at each scale. Therefore, the larger the uncertainties of the estimates, the smaller the influence of those estimates in the merging process. Moreover, the water body of the original MOD16 product is the fill values, and accordingly we did not estimate the LE of the water body when estimating the Landsat-based LE product. Note that some margins of the water body were assigned to certain values instead of fill values from the original products and even some abrupt changes were simultaneously produced around the water body in the merged MOD16, which were produced by spatial variability and scaling effects because all the child nodes were taken into account when transferred into the same parent nodes, not just a single pixel. Therefore, we propose that spatial variability and scaling effects cannot be ignored when merging two products at different spatial resolutions.

### C. Comparison of LE Products Before and After MRT

The two satellite products from 2005 and the corresponding merged results were compared. Fig. 7 shows that the histograms of the difference comparison between the MOD16 and the aggregated Landsat before and after the MRT. The distribution of the difference between the two satellite products was scattered with gray bars, and it was much more concentrated after data fusion. The bias was close to zero, and the difference was constrained to  $\pm 1$   $\text{W/m}^2$  in most cases, except for a few outliers. The absolute difference of the outliers that were larger than 20  $\text{W/m}^2$  was approximately 6%–7% before data fusion, while it dropped to lower than 1% after the MRT method.

Based on the statistical comparison (Table II) before and after the MRT method, the bias reduced by 38.3% on average. The more important improvement was that the RMSE significantly decreased by 49.2% on average compared with its original values. This indicates that the satellite products are more consistent and the lower RMSE (%) implies fewer outliers. These significant improvements show that the MRT method is capable of reducing the uncertainties

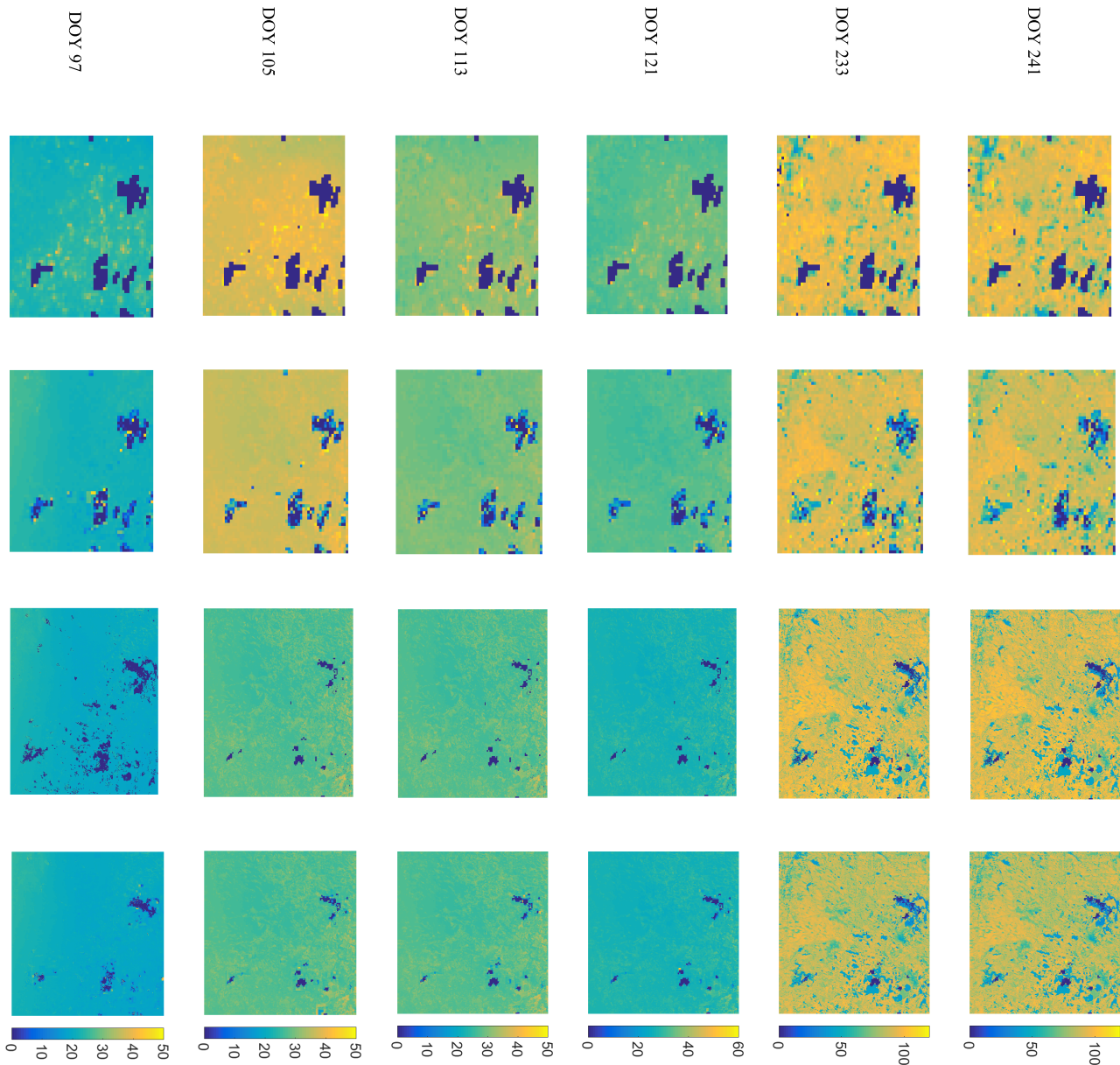


Fig. 6. Time series comparison before and after MRT. The order from top to bottom is the LE ( $W/m^2$ ) from original MODIS, the MODIS after MRT, the original Landsat, and the Landsat after MRT. The dark blue (0 value) means no data.

TABLE II  
COMPARISON BEFORE AND AFTER THE MRT (THE UNITS FOR BIAS AND RMSE ARE  $W/m^2$ )

Day	MODIS VS Aggregated Landsat					
	Before MRT			After MRT		
	Bias	RMSE	RMSE (%)	Bias	RMSE	RMSE (%)
97	2.364	6.866	31.234	1.462	3.763	17.353
105	8.003	12.928	36.462	7.330	8.358	24.036
113	1.404	8.397	29.098	0.812	3.982	14.092
121	4.198	9.920	31.343	3.599	5.081	16.363
233	2.683	24.418	29.264	1.466	10.832	13.161
241	1.631	24.050	29.192	0.295	10.244	12.628

of the satellite-based LE products and yielding consistent LE products at different scales.

In addition, Landsat and the MOD16 for estimating LE are mostly based on vegetation information, especially for the

Landsat-based LE product, which mainly depends on NDVI. Accordingly, the study area is mainly covered by vegetation. Hence, it is sensitive to the surface variation of LE and the fusion performance in the growing period is better than others. However, a few differences still exist. They might be caused by the actual differences between the physical structure of the algorithms for the two LE products and the effects of the sensor cloud residuals. It is worth noting that the performance of the data fusion in DOY 105 was not as significant as in other days. It also supports the expectation that the ability of the MRT method is limited when the preprocessing products have great differences.

Compared to the validations of the two LE products before the MRT method shown in Fig. 5, Fig. 8 illustrates the validations of the MRT-merged LE products versus the ground measurements. The RMSE of the merged Landsat LE

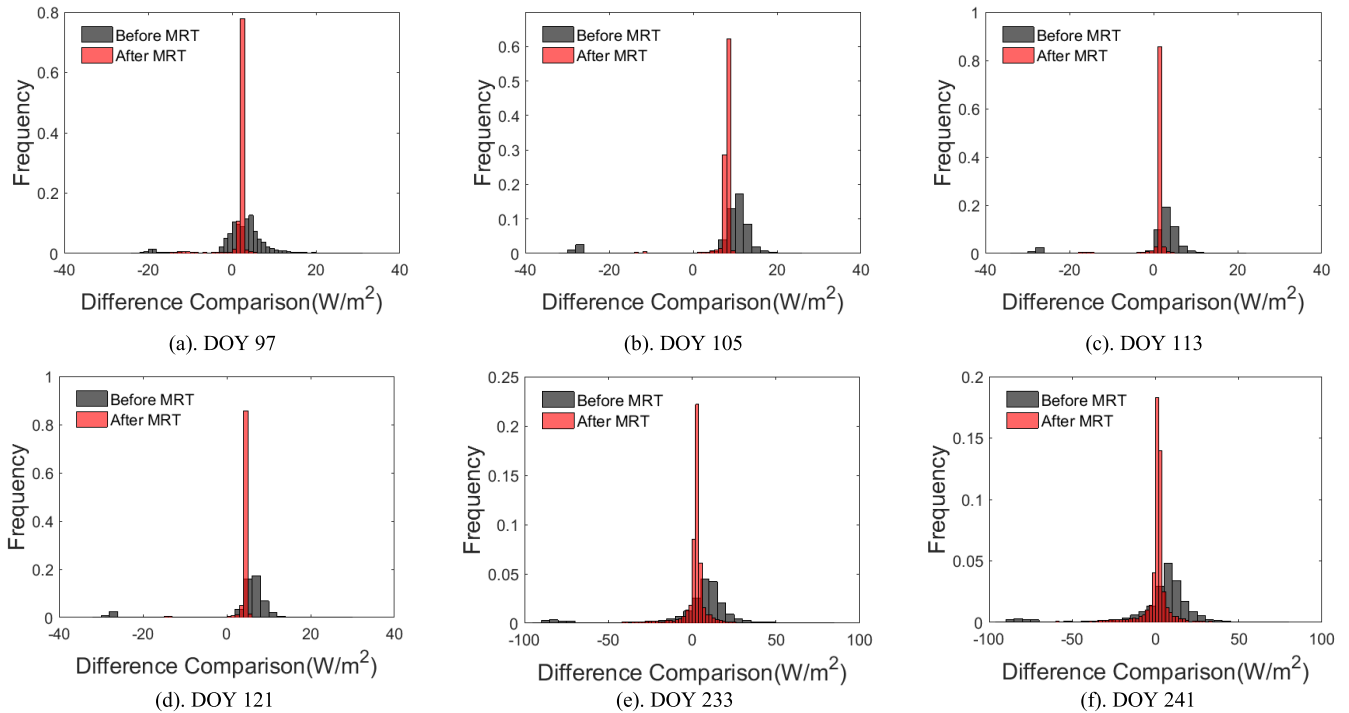


Fig. 7. Histograms of the differences comparison between the MOD16 and the aggregated Landsat before and after MRT. (a) DOY 97. (b) DOY 105. (c) DOY 113. (d) DOY 121. (e) DOY 233. (f) DOY 241.

product decreased from 17.317 to 14.689  $W/m^2$ , and the  $R^2$  improved from 0.866 to 0.897, which means that the merged Landsat product was more accurate after the MRT method. Similarly, the merged MOD16 was significantly improved with a decreasing RMSE from 27.6 to 19.739  $W/m^2$  and an increasing  $R^2$  from 0.626 to 0.794. Therefore, it simultaneously demonstrated that the MRT method is capable of improving the accuracies while eliminating the inconsistencies of the two LE products across different spatial resolutions. One notices that the improvement of the clear overestimation is more appreciable than that of the underestimation in the MOD16 because the slight underestimation of the Landsat data under the same conditions may be introduced to the MOD16.

## V. DISCUSSION

### A. Uncertainties of the Merged LE Estimates

1) *Errors in the Individual LE Products:* More than 80% of the study area is occupied by MF, DBF, and GRA in which the Landsat-based LE product has a higher  $R^2$  (0.7–0.8) than the  $R^2$  of the MOD16 (0.5–0.6) according to the validation of the ground measurements based on several hundred global sites [33]. The uncertainty of the two terrestrial LE products cannot be ignored. For example, Mu *et al.* [22] reported that the uncertainty of the MOD16 is up to 20% based on the individual point-based FLUXNET validation caused by the biases of the MERRA and the other inputs of the MODIS products [61]. Ershadi *et al.* [31] attributed the uncertainty of the MOD16 to the influence of the sensitivity of resistances parameterization of the PM algorithm. Ramoelo *et al.* [25] drew a similar conclusion that different sites or climatic zones lead to different performances of the MOD16 product. For the

Landsat-based LE product, the MERRA reanalysis data are a major data force for Landsat-based LE estimation. Recent studies have found large errors in the MERRA data [62], [63] and it tends to underestimate  $R_n$  at high values compared with the ground measurements, which may introduce substantial uncertainties into the LE estimation. Calibrating and adjusting the PT coefficients using the ground measurements at different vegetation types and climatic zones are recommended to reduce the errors of the LE estimation by 5%–25% [64].

2) *Scaling Effects:* The spatial scale mismatch between the EC ground measurements and the satellite products can directly affect the uncertainty in merged LE estimates. The EC flux tower is approximately several hundred meters [65]. Either the 30 m spatial resolution of the Landsat or the 900 m spatial resolution of the MOD16 product may not directly match the EC measurements and may even further increase the spatial differences. The evaluation of the merged LE products when ignoring spatial scaling effects may also lead to bias in the merged LEs. In addition, the abrupt changes around the water body of the merged results reflect the impact of scaling effects and the variability. To mitigate the scaling effects, spatial homogeneity of the study area with pure pixels is recommended.

3) *Biases of the EC Measurements:* The EC measurements are used as a reference to evaluate the uncertainty, but previous studies reported that the EC observed data have large uncertainties. For instance, there is currently no agreement on the interpretation of the reasons and the correction of the energy imbalance of EC measurements [66], [67]. EC measurements do not conserve energy, and the averaged energy closure at the five EC sites is 85%, which is mainly caused by the complexities of the wind patterns and the

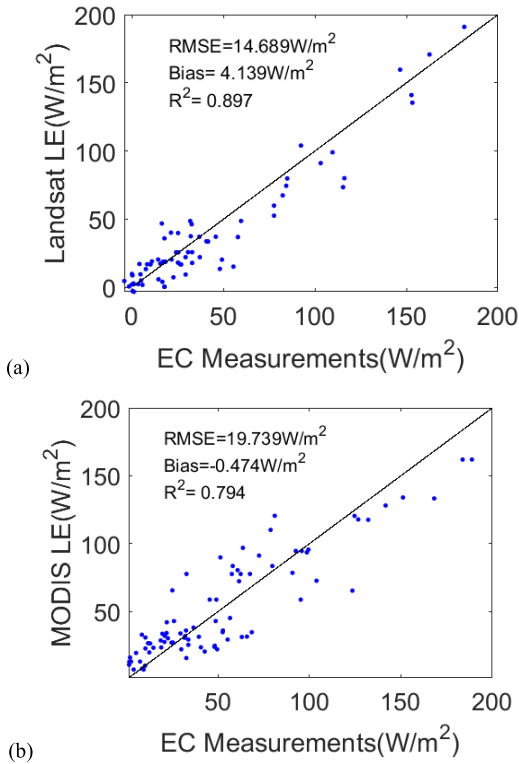


Fig. 8. Scatterplots of the validations of the MRT-merged LE products versus the ground measurements. (a) Landsat. (b) MOD16.

footprint variability [68]. In addition, it may be partially attributed to the fact that the EC method cannot capture large eddies in the lower boundary layer and measures only small eddies [11], [12]. Although several reasons for this energy closure problem have been documented by a substantial body of literature and we corrected for it in this paper, the errors produced by the correction and measurements are still unclear. The temporal upscaling from half hours to days may also introduce 5%–10% bias in the daily LE values [69] and the uncertainty of the EC measurements might further propagate to the fusion process. Hence, EC sites with fewer observed errors situated in the study area are conducive to precisely evaluating the uncertainty of the LE products.

4) *Fusion Method*: The weight values derived from the uncertainty evaluation using the EC ground measurements is shared by some subgrid pixels because the EC sites are too sparse in regions. The weight values analysis suggests a high dependence on dense EC sites in the study area. In addition, we postulate that the pixels at each scale have invariant errors within different temporal and spatial variations, and thus, the subsequent weighted values may not be adequately precise in the fusion process. The footprint model [70] concerns the relationship between the EC ground measurements and the spatial distance and can be used to estimate the accurate uncertainties of satellite products, which forms our next step.

#### B. Advantages and Limitations of the MRT Method

Compared to other merging methods, the MRT method shows three distinct superiorities. First, it has high computational efficiency. The MRT method only required 5.5 s in

our study, while the optimal interpolation method took several hours [36]. Second, the MRT method performs the capacity, which is not available in other merging methods such as the BMA method, to merge LE products at multiple resolutions and keep them consistent at each scale. The previous study showed that the MRT method also worked well in merging the albedo products at multiple spatial resolutions [71]. Finally, the MRT method can improve the accuracy of multiple LE products as well. The accuracy of the LE products increased by 15%–28% after the MRT method in this paper. Similar research reported by Jiang *et al.* [72] that the RMSE decreased from 1.30 to 0.45 compared to the reference map by the MRT method, when merging multiple LAI products. Overall, since the MRT method concentrates on data with multiple resolutions that carry more information, the accuracies of those products are considerably reinforced, and the merging images remain consistent at each scale, which satisfies the requirements of terrestrial satellite data fusion. We propose that other LE retrieving algorithms and other land surface modeling purposes can be better served by the MRT method as well.

Regardless of the excellent performance, the MRT method is also associated with three known limitations. First, it behaves relatively unpredictably when used with one input LE product that largely deviates from another. Shi *et al.* [60] drew a similar conclusion about the limitation of the MRT method when merging multiple broadband emissivity products. Second, the parameters of the MRT method are empirical and hard to predict, especially the state transition matrix from one scale to another. For instance, Gupta *et al.* [45] assumed that the state transition matrix is invariant across different scales, but Frakt and Willsky [73] stated that it depends on the parent-child cross-covariance and the state covariance. Finally, the basic assumption of the MRT method is that the data requires an expectation of zero mean at each scale. Currently, there is no agreement on the extraction of the spatial trend surface, and a variety of detrending methods have been previously implemented, such as spline fitting, the lognormal space [74], [75] and the power transformation [76], [77]. However, those methods suffer from either time-consuming computation [38] or full empirical parameterization. We used an average interpolation method to improve the efficiency in this paper, but it may lead to unpredictable performance for all the land cover types. Addressing these issues forms the foundation of our ongoing process.

## VI. CONCLUSION

Accurate LE estimation at high spatial and temporal resolutions is essential in evaluating the surface energy balance. Currently, the uncertainties of individual satellite-based LE products are mainly derived from systematic sensor errors, contaminated clouds, angular composition, and the physical differences among the LE retrieving algorithms. To reduce the errors and improve the accuracy of the LE products, it is important to take full advantage of multiple LE products. This paper applies a novel approach to merge satellite-based LE products at different spatiotemporal resolutions.

This paper uses the MRT method to merge the Landsat-based LE product and the MOD16 product with the main purpose of improving the consistency between different LE products across different resolutions. To the best of our knowledge, this is the first time that the MRT method has been applied on satellite-based LE products.

The fusion results prove that the MRT method is capable of reducing the inconsistency, improving the accuracy, and generating consistent LE products among LE products at different spatial scales. Therefore, we propose that the MRT method has the potential to estimate other essential land surface products with similar problems in other areas.

The MRT method is currently limited to several land cover types and homogeneous pixels. This paper simplifies the underlying surface of the study area and not all types of surface coverage are represented. Since the merging performance is greatly affected by the uncertainties of the LE products, the EC ground measurements we used may not actually evaluate the real error of each product. Our next step is to extensively and precisely evaluate the errors of the LE products at regional scales to make the MRT method more universal.

#### APPENDIX MS-PT ALGORITHM

The modified satellite-based PT (MS-PT) algorithm was developed by Yao *et al.* [54] and was calculated as the sum of the unsaturated soil evaporation ( $LE_s$ ), the saturated wet soil surface evaporation ( $LE_{ws}$ ), the canopy transpiration ( $LE_c$ ), and the canopy interception evaporation ( $LE_{ic}$ ). It can be expressed as follows:

$$LE = LE_s + LE_{ws} + LE_c + LE_{ic} \quad (A1)$$

$$LE_s = \partial(1 - f_{wet})f_{sm} \frac{\Delta}{\Delta + \gamma} (R_{ns} - G) \quad (A2)$$

$$LE_{ws} = \partial f_{wet} \frac{\Delta}{\Delta + \gamma} (R_{ns} - G) \quad (A3)$$

$$LE_c = \partial(1 - f_{wet})f_c f_T \frac{\Delta}{\Delta + \gamma} R_{nc} \quad (A4)$$

$$LE_{ic} = \partial f_{wet} \frac{\Delta}{\Delta + \gamma} R_{nc} \quad (A5)$$

$$f_{sm} = AT_1^k = \left( \frac{1}{DT} \right)^{DT/DT_{max}} \quad (A6)$$

$$f_{wet} = f_{sm}^4 \quad (A7)$$

$$f_c = \frac{NDVI - NDVI_{min}}{NDVI_{max} - NDVI_{min}} \quad (A8)$$

where  $DT_{max}$  is the maximum diurnal air temperature range (40 °C) and  $f_c$  is vegetation cover fraction.  $NDVI_{min}$  and  $NDVI_{max}$  are the minimum and maximum of the NDVI and are set as 0.05 and 0.95 [78] in this algorithm, respectively.

#### ACKNOWLEDGMENT

The authors would like to thank Prof. J. Chen from Michigan State University, East Lansing, MI, USA, for his suggestions to improve this paper. They would like to thank the California Institute of Technology and Government Sponsorship. J. B. Fisher contributed to this paper from the Jet

Propulsion Laboratory, California Institute of Technology, under a contract with the National Aeronautics and Space Administration. Copyright 2018. All rights reserved.

#### REFERENCES

- [1] J. L. Monteith, "Evaporation and environment," in *Proc. Symp. Soc. Experm. Biol.*, 1965, vol. 19, no. 19, p. 205.
- [2] J. D. Kalma, T. R. McVicar, and M. F. McCabe, "Estimating land surface evaporation: A review of methods using remotely sensed surface temperature data," *Surv. Geophys.*, vol. 29, no. 4, pp. 421–469, Oct. 2008.
- [3] S. Liang, K. Wang, X. Zhang, and M. Wild, "Review on estimation of land surface radiation and energy budgets from ground measurement, remote sensing and model simulations," *IEEE J. Sel. Topics Appl. Earth Observ. Remote Sens.*, vol. 3, no. 3, pp. 225–240, Sep. 2010.
- [4] K. Wang and R. E. Dickinson, "A review of global terrestrial evapotranspiration: Observation, modeling, climatology, and climatic variability," *Rev. Geophys.*, vol. 50, no. 2, p. RG2005, Jun. 2012.
- [5] J. B. Fisher *et al.*, "The future of evapotranspiration: Global requirements for ecosystem functioning, carbon and climate feedbacks, agricultural management, and water resources," *Water Resour. Res.*, vol. 53, no. 4, pp. 2618–2626, 2017.
- [6] K. Mallick *et al.*, "Latent heat flux estimation in clear sky days over Indian agroecosystems using noontime satellite remote sensing data," *Agricult. Forest Meteorol.*, vol. 149, no. 10, pp. 1646–1665, Oct. 2015.
- [7] W. Yuan *et al.*, "Global estimates of evapotranspiration and gross primary production based on MODIS and global meteorology data," *Remote Sens. Environ.*, vol. 114, no. 7, pp. 1416–1431, 2010.
- [8] I. S. Bowen, "The ratio of heat losses by conduction and by evaporation from any water surface," *Phys. Rev.*, vol. 27, no. 6, pp. 779–787, 1926.
- [9] D. Cook, "Energy balance bowen ratio station (EBBR) handbook," Office Sci. Tech. Inf., Tech. Rep., 2011.
- [10] D. E. Angus and P. J. Watts, "Evapotranspiration—How good is the Bowen ratio method?" *Agricult. Water Manage.*, vol. 8, nos. 1–3, pp. 133–150, Jan. 1984.
- [11] K. Wilson *et al.*, "Energy balance closure at FLUXNET sites," *Agricult. Forest Meteorol.*, vol. 113, nos. 1–4, pp. 223–243, 2002.
- [12] T. Foken, "The energy balance closure problem: An overview," *Ecol. Soc. Amer.*, vol. 18, no. 6, pp. 1351–1367, 2008.
- [13] C. Beer *et al.*, "Terrestrial gross carbon dioxide uptake: Global distribution and covariation with climate," *Science*, vol. 329, no. 5993, pp. 834–838, Aug. 2010.
- [14] T. Xu, S. Liu, S. Liang, and J. Qin, "Improving predictions of water and heat fluxes by assimilating MODIS land surface temperature products into the common land model," *J. Hydrometeorol.*, vol. 12, no. 2, pp. 227–244, 2010.
- [15] Y. Yao *et al.*, "A satellite-based hybrid algorithm to determine the Priestley–Taylor parameter for global terrestrial latent heat flux estimation across multiple biomes," *Remote Sens. Environ.*, vol. 165, pp. 216–233, Aug. 2015.
- [16] D. Baldocchi *et al.*, "FLUXNET: A new tool to study the temporal and spatial variability of ecosystem-scale carbon dioxide, water vapor, and energy flux densities," *Bull. Amer. Meteorol. Soc.*, vol. 82, no. 82, pp. 2415–2434, 2001.
- [17] S. Liu *et al.*, "Upscaling evapotranspiration measurements from multi-site to the satellite pixel scale over heterogeneous land surfaces," *Agricult. Forest Meteorol.*, vols. 230–231, pp. 97–113, Dec. 2016.
- [18] H. Fang, S. Liang, J. R. Townshend, and R. E. Dickinson, "Spatially and temporally continuous LAI data sets based on an integrated filtering method: Examples from North America," *Remote Sens. Environ.*, vol. 112, no. 1, pp. 75–93, Jan. 2008.
- [19] C. Jiménez *et al.*, "Global intercomparison of 12 land surface heat flux estimates," *J. Geophys. Res. Atmos.*, vol. 116, no. D2, pp. 3–25, 2010.
- [20] Y. Yao *et al.*, "A simple temperature domain two-source model for estimating agricultural field surface energy fluxes from Landsat images," *J. Geophys. Res.*, vol. 122, no. 10, pp. 5211–5236, May 2017.
- [21] Q. Mu, F. A. Heinsch, M. Zhao, and S. W. Running, "Development of a global evapotranspiration algorithm based on MODIS and global meteorology data," *Remote Sens. Environ.*, vol. 111, no. 4, pp. 519–536, Dec. 2007.
- [22] Q. Mu, M. Zhao, and S. W. Running, "Improvements to a MODIS global terrestrial evapotranspiration algorithm," *Remote Sens. Environ.*, vol. 115, no. 8, pp. 1781–1800, 2011.
- [23] Y. Chen *et al.*, "Comparison of satellite-based evapotranspiration models over terrestrial ecosystems in China," *Remote Sens. Environ.*, vol. 140, no. 140, pp. 279–293, Jan. 2014.

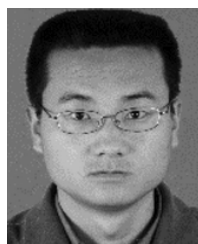
- [24] J. B. Fisher, K. P. Tu, and D. D. Baldocchi, "Global estimates of the land-atmosphere water flux based on monthly AVHRR and ISLSCP-II data, validated at 16 FLUXNET sites," *Remote Sens. Environ.*, vol. 112, no. 3, pp. 901–919, Mar. 2008.
- [25] A. Ramoelo, N. Majazi, R. Mathieu, N. Jovanovic, A. Nickless, and S. Dzikioti, "Validation of global evapotranspiration product (MOD16) using flux tower data in the African savanna, South Africa," *Remote Sens.*, vol. 6, no. 8, pp. 7406–7423, 2014.
- [26] H. W. Kim, K. Hwang, Q. Mu, S. O. Lee, and M. Choi, "Validation of MODIS 16 global terrestrial evapotranspiration products in various climates and land cover types in Asia," *KSCE J. Civil Eng.*, vol. 16, no. 2, pp. 229–238, 2012.
- [27] J. Ju and D. P. Roy, "The availability of cloud-free Landsat ETM+ data over the conterminous United States and globally," *Remote Sens. Environ.*, vol. 112, no. 3, pp. 1196–1211, Mar. 2008.
- [28] Q. Tang, E. A. Rosenberg, and D. P. Lettenmaier, "Use of satellite data to assess the impacts of irrigation withdrawals on Upper Klamath Lake, Oregon," *Hydrol. Earth Syst. Sci.*, vol. 13, no. 1, pp. 617–627, 2009.
- [29] M. C. Anderson, R. G. Allen, A. Morse, and W. P. Kustas, "Use of Landsat thermal imagery in monitoring evapotranspiration and managing water resources," *Remote Sens. Environ.*, vol. 122, no. 1, pp. 50–65, Jul. 2012.
- [30] N. Bhattarai, L. J. Quackenbush, M. Dougherty, and L. J. Marzen, "A simple Landsat–MODIS fusion approach for monitoring seasonal evapotranspiration at 30 m spatial resolution," *Int. J. Remote Sens.*, vol. 36, no. 1, pp. 115–143, 2015.
- [31] A. Ershadi, M. F. McCabe, J. P. Evans, N. W. Chaney, and E. F. Wood, "Multi-site evaluation of terrestrial evaporation models using FLUXNET data," *Agricult. Forest Meteorol.*, vol. 187, no. 8, pp. 46–61, Apr. 2014.
- [32] Q. Duan, N. K. Ajami, X. Gao, and S. Sorooshian, "Multi-model ensemble hydrologic prediction using Bayesian model averaging," *Adv. Water Resour.*, vol. 30, no. 5, pp. 1371–1386, May 2007.
- [33] Y. Yao *et al.*, "Bayesian multimodel estimation of global terrestrial latent heat flux from eddy covariance, meteorological, and satellite observations," *J. Geophys. Res. Atmos.*, vol. 119, no. 8, pp. 4521–4545, 2014.
- [34] G. Zhu *et al.*, "Multi-model ensemble prediction of terrestrial evapotranspiration across north China using Bayesian model averaging," *Hydrol. Process.*, vol. 30, no. 16, pp. 2861–2879, 2016.
- [35] F. Feng *et al.*, "An empirical orthogonal function-based algorithm for estimating terrestrial latent heat flux from eddy covariance, meteorological and satellite observations," *PLoS ONE*, vol. 11, no. 7, p. e0160150, 2016.
- [36] D. Wang and S. Liang, "Using multiresolution tree to integrate MODIS and MISR-L3 LAI products," in *Proc. IEEE Int. Geosci. Remote Sens. Symp.*, Jul. 2010, vol. 38, no. 5, pp. 1027–1030.
- [37] K. C. Chou, A. S. Willsky, and R. Nikoukhah, "Multiscale systems, Kalman filters, and Riccati equations," *IEEE Trans. Autom. Control*, vol. 39, no. 3, pp. 479–492, Mar. 1994.
- [38] W. Yue and J. Zhu, "On estimation and prediction for multivariate multiresolution tree-structured spatial linear models," *Statist. Sinica*, vol. 16, no. 3, pp. 981–1020, 2006.
- [39] S. Liang *et al.*, "Methodologies for integrating multiple high-level remotely sensed land products," in *Comprehensive Remote Sensing*, 2018, pp. 278–317.
- [40] X. Tao, S. Liang, D. Wang, T. He, and C. Huang, "Improving satellite estimates of the fraction of absorbed photosynthetically active radiation through data integration: Methodology and validation," *IEEE Trans. Geosci. Remote Sens.*, vol. 56, no. 4, pp. 2107–2118, Apr. 2018.
- [41] L. M. Parada and X. Liang, "Optimal multiscale Kalman filter for assimilation of near-surface soil moisture into land surface models," *J. Geophys. Res. Atmos.*, vol. 109, no. D24, Dec. 2004.
- [42] H.-C. Huang, N. Cressie, and J. Gabrosek, "Fast, resolution-consistent spatial prediction of global processes from satellite data," *J. Comput. Graph. Statist.*, vol. 11, no. 1, pp. 63–88, 2002.
- [43] M. R. Luetzgen and A. S. Willsky, "Likelihood calculation for a class of multiscale stochastic models, with application to texture discrimination," *IEEE Trans. Image Process.*, vol. 4, no. 2, pp. 194–207, 1995.
- [44] S. Tzeng, H.-C. Huang, and N. Cressie, "A fast, optimal spatial-prediction method for massive datasets," *Amer. Statist. Assoc.*, vol. 100, no. 472, pp. 1343–1357, 2005.
- [45] R. Gupta, V. Venugopal, and E. Foufoula-Georgiou, "A methodology for merging multisensor precipitation estimates based on expectation-maximization and scale-recursive estimation," *J. Geophys. Res. Atmos.*, vol. 111, no. D2, 2015.
- [46] P. W. Fieguth, W. C. Karl, and A. S. Willsky, "Multiresolution optimal interpolation and statistical analysis of TOPEX/POSEIDON satellite altimetry," *IEEE Trans. Geosci. Remote Sens.*, vol. 33, no. 2, pp. 280–292, Mar. 1995.
- [47] A. Kannan, M. Ostendorf, W. C. Karl, D. A. Castanon, and R. K. Fish, "ML parameter estimation of a multiscale stochastic process using the EM algorithm," *IEEE Trans. Signal Process.*, vol. 48, no. 6, pp. 1836–1840, Jun. 2000.
- [48] H. V. D. Vyver and E. Roulin, "Scale-recursive estimation for merging precipitation data from radar and microwave cross-track scanners," *J. Geophys. Res. Atmos.*, vol. 114, no. D8, pp. D08104–D08117, 2009.
- [49] M. A. Friedl *et al.*, "MODIS collection 5 global land cover: Algorithm refinements and characterization of new datasets," *Remote Sens. Environ.*, vol. 114, no. 1, pp. 168–182, Jan. 2010.
- [50] T. E. Twine *et al.*, "Correcting eddy-covariance flux underestimates over a grassland," *Agricult. Forest Meteorol.*, vol. 103, no. 3, pp. 279–300, 2000.
- [51] H. A. Cleugh, R. Leuning, Q. Mu, and S. W. Running, "Regional evaporation estimates from flux tower and MODIS satellite data," *Remote Sens. Environ.*, vol. 106, no. 3, pp. 285–304, Feb. 2007.
- [52] E. J. Kirkland, *Bilinear Interpolation*. New York, NY, USA: Springer, 2010, pp. 261–263.
- [53] J. G. Masek *et al.*, "A Landsat surface reflectance dataset for North America, 1990–2000," *IEEE Geosci. Remote Sens. Lett.*, vol. 3, no. 1, pp. 68–72, Jan. 2006.
- [54] Y. Yao *et al.*, "MODIS-driven estimation of terrestrial latent heat flux in China based on a modified Priestley–Taylor algorithm," *Agricult. Forest Meteorol.*, vols., 171–172, no. 3, pp. 187–202, Apr. 2013.
- [55] C. H. B. Priestley and R. J. Taylor, "On the assessment of surface heat flux and evaporation using large-scale parameters," *Monthly Weather Rev.*, vol. 100, no. 2, pp. 81–92, 2009.
- [56] M. Zhao, F. A. Heinsch, R. R. Nemani, and S. W. Running, "Improvements of the MODIS terrestrial gross and net primary production global data set," *Remote Sens. Environ.*, vol. 95, no. 2, pp. 164–176, Mar. 2005.
- [57] A. K. Betts, M. Zhao, P. A. Dirmeyer, and A. C. M. Beljaars, "Comparison of ERA40 and NCEP/DOE near-surface data sets with other ISLSCP-II data sets," *J. Geophys. Res. Atmos.*, vol. 111, no. D22, 2006.
- [58] C. A. Schlosser and X. Gao, "Assessing evapotranspiration estimates from the second global soil wetness project (GSWP-2) simulations," *Rep.-MIT Joint Program Sci. Policy Global Change*, vol. 11, no. 4, pp. 880–897, 2009.
- [59] J. Liu *et al.*, "Validation of Moderate Resolution Imaging Spectroradiometer (MODIS) albedo retrieval algorithm: Dependence of albedo on solar zenith angle," *J. Geophys. Res. Atmos.*, vol. 114, no. D1, 2009.
- [60] L. Shi, S. Liang, J. Cheng, and Q. Zhang, "Integrating ASTER and GLASS broadband emissivity products using a multi-resolution Kalman filter," *Int. J. Digit. Earth*, vol. 9, no. 11, pp. 1098–1116, 2016.
- [61] N. M. Velpuri, G. B. Senay, R. K. Singh, S. Bohms, and J. P. Verdin, "A comprehensive evaluation of two MODIS evapotranspiration products over the conterminous United States: Using point and gridded FLUXNET and water balance ET," *Remote Sens. Environ.*, vol. 139, no. 4, pp. 35–49, 2013.
- [62] M. Zhao, S. W. Running, and R. R. Nemani, "Sensitivity of Moderate Resolution Imaging Spectroradiometer (MODIS) terrestrial primary production to the accuracy of meteorological reanalyses," *J. Geophys. Res. Biogeosci.*, vol. 111, no. G1, pp. 338–356, 2006.
- [63] M. Bosilovich *et al.*, "NASA's modern era retrospective-analysis for research and applications (MERRA)," in *Proc. AGU Fall Meeting*, 2010, pp. 431–434.
- [64] M. C. Anderson, J. M. Norman, W. P. Kustas, R. Houborg, P. J. Starks, and N. Agam, "A thermal-based remote sensing technique for routine mapping of land-surface carbon, water and energy fluxes from field to regional scales," *Remote Sens. Environ.*, vol. 112, no. 12, pp. 4227–4241, Dec. 2008.
- [65] M. F. McCabe and E. F. Wood, "Scale influences on the remote estimation of evapotranspiration using multiple satellite sensors," *Remote Sens. Environ.*, vol. 105, no. 4, pp. 271–285, Dec. 2006.
- [66] G. Wohlfahrt *et al.*, "On the consequences of the energy imbalance for calculating surface conductance to water vapour," *Agricult. Forest Meteorol.*, vol. 149, no. 9, pp. 1556–1559, 2009.
- [67] R. Leuning, G. van Gorsel, W. J. Massman, and P. R. Isaac, "Reflections on the surface energy imbalance problem," *Agricult. Forest Meteorol.*, vol. 156, no. 156, pp. 65–74, Apr. 2012.
- [68] K. Zhang, J. S. Kimball, R. R. Nemani, and S. W. Running, "A continuous satellite-derived global record of land surface evapotranspiration from 1983 to 2006," *Water Resour. Res.*, vol. 46, no. 9, pp. 109–118, 2010.

- [69] D. Hui, S. Wan, B. Su, G. Katul, R. Monson, and Y. Luo, "Gap-filling missing data in eddy covariance measurements using multiple imputation (MI) for annual estimations," *Agricult. Forest Meteorol.*, vol. 121, nos. 1–2, pp. 93–111, Jan. 2004.
- [70] Z. Jia, S. Liu, Z. Xu, Y. Chen, and M. Zhu, "Validation of remotely sensed evapotranspiration over the Hai River Basin, China," *J. Geophys. Res. Atmos.*, vol. 117, no. D13, 2012.
- [71] T. He, S. Liang, D. Wang, Y. Shuai, and Y. Yu, "Fusion of satellite land surface albedo products across scales using a multiresolution tree method in the North Central United States," *IEEE Trans. Geosci. Remote Sens.*, vol. 52, no. 6, pp. 3428–3439, Jun. 2014.
- [72] J. Jiang, Z. Xiao, J. Wang, and J. Song, "Multiscale estimation of leaf area index from satellite observations based on an ensemble multiscale filter," *Remote Sens.*, vol. 8, no. 3, p. 229, 2016.
- [73] A. B. Frakt and A. S. Willsky, "Computationally efficient stochastic realization for internal multiscale autoregressive models," *Multidimensional Syst. Signal Process.*, vol. 12, no. 2, pp. 109–142, 2001.
- [74] B. Tustison, E. Foufoula-Georgiou, and D. Harris, "Scale-recursive estimation for multisensor Quantitative Precipitation Forecast verification: A preliminary assessment," *J. Geophys. Res. Atmos.*, vol. 107, no. D8, pp. CIP-1–CIP 2-14, 2002.
- [75] I. P. Gorenburg, D. McLaughlin, and D. Entekhabi, "Scale-recursive assimilation of precipitation data," *Adv. Water Resour.*, vol. 24, nos. 9–10, pp. 941–953, 2001.
- [76] Q. Y. Duan, V. K. Gupta, and S. Sorooshian, *Shuffled Complex Evolution Approach for Effective and Efficient Global Minimization*. New York, NY, USA: Plenum, 1993, pp. 501–521.
- [77] H. V. D. Vyver and E. Roulin, "Scale-recursive estimation for merging precipitation data from radar and microwave cross-track scanners," *J. Geophys. Res. Atmos.*, vol. 114, no. D8, 2009.
- [78] K. Zhang, J. S. Kimball, Q. Mu, L. A. Jones, S. J. Goetz, and S. W. Running, "Satellite based analysis of northern ET trends and associated changes in the regional water balance from 1983 to 2005," *J. Hydrol.*, vol. 379, nos. 1–2, pp. 92–110, Dec. 2009.



**Jia Xu** received the B.E. degree in spatial information and digital technology from the University of Electronic Science and Technology of China, Chengdu, China, in 2016. She is currently pursuing the M.S. degree in cartography and geographical information system with the State Key Laboratory of Remote Sensing Science, Faculty of Geographical Science, Beijing Normal University, Beijing, China.

Her research interests include retrieval and estimation of land surface evapotranspiration by remote sensing.



**Yunjun Yao** received the Ph.D. degree from Peking University, Beijing, China, in 2010.

From 2008 to 2009, he was a Joint Ph.D. Student with the Department of Geographical Sciences, University of Maryland, College Park, MD, USA. He is currently with the State Key Laboratory of Remote Sensing Science, Faculty of Geographical Science, Beijing Normal University, Beijing, China. His research interests include the estimation of evapotranspiration and retrieval of surface biophysical parameters by remote sensing.



**Shunlin Liang** (M'94–F'13) received the Ph.D. degree from Boston University, Boston, MA, USA.

He is currently a Professor with the Department of Geographical Sciences, University of Maryland, College Park, MD, USA. His research interests include the estimation of land surface variables from satellite data, earth energy balance, and assessment of environmental changes. He has authored over 270 SCI indexed peer-reviewed journal papers and the book *Quantitative Remote Sensing of Land Surfaces* (Wiley, 2004), co-authored the book *Global Land Surface Satellite Products: Algorithms, Validation and Analysis* (Springer, 2013), edited the book *Advances in Land Remote Sensing: System, Modeling, Inversion and Application* (Springer, 2008), and co-edited the books *Advanced Remote Sensing: Terrestrial Information Extraction and Applications* (Academic Press, 2012) and *Land Surface Observation, Modeling and Data Assimilation* (World Scientific, 2013).

Dr. Liang was an Associate Editor of the IEEE TRANSACTION ON GEOSCIENCE AND REMOTE SENSING and also a Guest Editor of several remote sensing related journals.



**Shaomin Liu** received the B.S. degree in agricultural meteorology and the M.S. degree in applied meteorology from the Nanjing Institute of Meteorology, Nanjing, China, in 1988 and 1991, respectively, and the Ph.D. degree in ecology from China Agricultural University, Beijing, China, in 2001.

He is currently a Professor with the State Key Laboratory of Earth Surface Processes and Resource Ecology and the Faculty of Geographical Science, Beijing Normal University, Beijing. He has authored over 100 scientific papers, including over 70 SCI

papers and four ESI highly cited papers. His research interests include hydrometeorology and remote sensing.



**Joshua B. Fisher** received the B.S. degree in environmental sciences and the Ph.D. degree in environmental science, policy, and management from the University of California, Berkeley, CA, USA, in 2001 and 2006, respectively.

He was a Post-Doctoral Researcher at the University of Oxford, Oxford, U.K. He joined the NASA's Jet Propulsion Laboratory, Pasadena, CA, USA, in 2010. He is currently the Science Lead of the ECOSTRESS mission, where he focused on evapotranspiration. He was involved in ecosystem

modeling for over 10 years, developed new models of hydrological and nutrient cycling, conducted large-scale field campaigns to gather data to parameterize and test models, modeling and field work, while integrating a wide range of measurement techniques such as eddy covariance and remote sensing.



**Kun Jia** received the B.S. degree in surveying and mapping engineering from Central South University, Changsha, China, in 2006, and the Ph.D. degree in cartography and geographic information system from the Institute of Remote Sensing Applications, Chinese Academy of Sciences, Beijing, China, in 2011.

He is currently an Associate Professor with the State Key Laboratory of Remote Sensing Science, Faculty of Geographical Science, Beijing Normal University, Beijing. His research interests include

the estimation of fractional vegetation cover, land cover classification, and agriculture monitoring using remote sensing data.



**Xiaotong Zhang** received the Ph.D. degree in cartography and geographical information science from Wuhan University, Wuhan, China, in 2010.

He was a Joint Ph.D. Student with the Department of Geographical Sciences, University of Maryland, College Park, MD, USA. He is currently with the State Key Laboratory of Remote Sensing Science, Faculty of Geographical Science, Beijing Normal University, Beijing, China. His research interests include the estimation of land surface radiation components from satellite data, and earth energy balance.



**Lilin Zhang** is currently pursuing the M.S. degree in cartography and geographical information system with the State Key Laboratory of Remote Sensing Science, Faculty of Geographical Science, Beijing Normal University, Beijing, China.

His research interests include evapotranspiration and agricultural drought monitoring.



**Yi Lin** received the Ph.D. degree in photogrammetry and remote sensing from Peking University, Beijing, China, in 2009.

From 2009 to 2012, he was a Senior Research Scientist with the Department of Remote Sensing and Photogrammetry, Finnish Geodetic Institute, Masala, Finland. He is currently a Research Professor with the School of Earth and Space Sciences, Peking University. He has authored or co-authored over 50 refereed papers. His research interests include LiDAR remote sensing, earth interaction, and earth observation.



**Xiaowei Chen** is currently pursuing the M.S. degree in cartography and geographical information system the State Key Laboratory of Remote Sensing Science, Faculty of Geographical Science, Beijing Normal University, Beijing, China.

Her research interests include sensible and latent heat flux in ocean by remote sensing and reanalysis products.